Available online at www.sciencedirect.com
SCIENCE DIRECT®
European Journal of Pharmaceutical Sciences 18 (2003) 313–322
EUROPEAN JOURNAL OF PHARMACEUTICAL SCIENCES
www.elsevier.com/locate/ejps

Reversible and irreversible inhibitory activity of succinic and maleic acid derivatives on acetylcholinesterase

J. Trujillo-Ferrara[a,*], Iván Vázquez[a], Judith Espinosa[a], Rosa Santillan[b], Norberto Farfán[b], Herbert Höpfl[c]

[a]*Sección de Graduados y Departamento de Bioquímica, Escuela Superior de Medicina, Instituto Politécnico Nacional, Plan de San Luis y Díaz Mirón, México, D.F. 11340, Mexico*
[b]*Departamento de Química del Centro de Investigación y Estudios Avanzados, Instituto Politécnico Nacional, Apartado Postal 14-740, México, D.F. 07000, Mexico*
[c]*Universidad Autónoma del Estado de Morelos, Centro de Investigaciones Químicas, Av. Universidad 1001, CP 62210 Cuernavaca, Morelos, Mexico*

Received 11 September 2002; received in revised form 3 February 2003; accepted 3 February 2003

Abstract

Aryl succinic and maleic acid derivatives are potent inhibitors of bovine acetylcholinesterase in vitro. Succinic acid aminophenol derivatives **1**b–e and **2**b–d act as reversible inhibitors of acetylcholinesterase, while maleic acid aminophenol derivatives **3**b–d and **4**c–e act as choline subsite-directed irreversible inhibitors, detected by dialysis in the presence of edrophonium. Linear relationships between the logarithm of the velocity of hydrolysis of acetylcholine plotted against the time of incubation at several different inhibitor concentrations were determined. The K_i for reversible competitive inhibitors was determined. For irreversible inhibitors the K_i for the dissociation constant of the enzyme–inhibitor complex at the beginning of the recognition process was also determined as well as the inactivation constant of the enzyme–inhibitor adduct formation k_{+2} and the bimolecular inhibition constant k_i for the inhibition of acetylcholinesterase by aminophenol derivatives **3**b–d and **4**c–e. The conclusions of this study can be summarized as follows for both families: (a) the aromatic moiety played a critical role in the recognition of the active site; (b) in case of the reversible inhibitor, when the ester function took the place of the hydroxyl fragment, there was an important increase in the affinity; and (c) the distance between phenolic hydroxyl and nitrogen was critical because the inhibition is *ortho* ≪ *meta* < *para*.

Keywords: Acetylcholine; Acetylcholinesterase; Succinic and maleic acids; Reversible and irreversible inhibitors

1. Introduction

Acetylcholine (ACh) is an important neurotransmitter across nerve–nerve and neuromuscular synapses in both the central and the peripheral nervous system. Acetylcholinesterase (AChE, EC 3.1.1.7) ends the ACh action by its hydrolysis of it (Quinn, 1987).

Today it is well known that senile dementia of the Alzheimer's type is a neurodegenerative disease consistent with low concentrations of cholinergic markers such as ACh and cholinetransferase (Taylor, 1998, 2001; Trybulski et al., 1992). Therefore, the development of potent and specific AChE inhibitors with low toxicity that cause increasing ACh levels in the affected regions of the brain might lead to a better understanding of the pathology of this disease and permit the emergence of effective therapeutic modalities. In general, compounds containing a quaternary ammonium group do not penetrate the cell membrane; hence, anti-AChE agents in this category are absorbed poorly from the gastrointestinal tract or through the skin and are excluded from the central nervous system by the blood–brain barrier (Berman and Leonard, 1991; Taylor, 2001). In contrast, the more lipid soluble agents are well absorbed after oral administration and have ubiquitous effects at both peripheral and central cholinergic sites.

Molecular cloning revealed that a single gene encodes vertebrates. However, multiple genes encode in other biological systems; this diversity arises from alternative processing of the mRNA. The different forms differ only in their carboxyl-termini; the portion of the gene that encodes the catalytic core of the enzyme is invariant

*Corresponding author. Fax: +52-555-729-6000x62744.
E-mail address: jtrujillo@ipn.mx (J. Trujillo-Ferrara).

0928-0987/03/$ – see front matter
doi:10.1016/S0928-0987(03)00023-X

(Schumacher et al., 1986; Grisaru et al., 1999; Taylor, 2001).

In 1991 the molecular structure of AChE from *Torpedo californica* (TcAChE) was examined by X-ray crystallography (Sussman et al., 1991), and in 1995 the three dimensional structure *mouse* AChE (mAChE) was examined in a complex with fasciculin 2 (Fas 2) (Bourne et al., 1995) and only slight differences were observed in the conformation of Fas2-associated mAChE compared with uncomplexed TcAChE. The active site of mAChE consists of: (a) a steratic site (ES) that is comprised of the catalytic triad Ser203, His447 and Glu334; (b) an acyl binding site (ABS) located on Phe295 and Phe297, that binds the acetyl group of ACh and that is important for binding interactions with aryl substrates and active site ligands (Lin et al., 1999); (c) a choline subsite with Trp86, Glu202 and Tyr337 that contains a small number of negative charges, but many aromatic residues, and where the quaternary ammonium pole of ACh and various active site ligands bind through a preferential interaction of quaternary nitrogens with the π electrons of the aromatic groups; (d) a peripheral anionic binding site (PAS), consisting of Trp286, Tyr72, Tyr124 and Asp74. Tyrosines 337 and 449 are further removed from the active center but likely contribute to the stabilization of certain ligands.

A step forward into the treatment of Alzheimer's disease has involved attempts to augment the cholinergic function of the brain. A somewhat more successful strategy has been the use of inhibitors of AChE. Nowadays new inhibitors can be developed by molecular design strategies in order to take advantage of several important features of the active-site gorge of AChE so that a drug can be produced with both a high affinity and a high degree of selectivity for the enzyme (Recatini et al., 1997; Kryger et al., 1999).

In this paper we report the in vitro inhibition of AChE by a variety of carefully designed amide and imide derivatives of succinic and maleic acids (Fig. 1) that have been previously synthesized in our laboratory (Trujillo-Ferrara et al., 1999). Four of them are new compounds (**1**d, **2**d, **3**d and **4**e; Fig. 2) and a complete characterization of ^{1}H and ^{13}C NMR spectroscopy is reported.

Before the design of the inhibitors we considered several factors that would be important for an optimum activity (Baker and Alumaula, 1963). Firstly, there should be a structural relationship between ACh, choline (Ch) and the inhibitors. Secondly, most of the ligands were prepared from aromatic starting materials in order to enhance the selectivity of molecular recognition on the surface of the active site gorge, which contains 40% of aromatic residues (Sussman et al., 1991). The structural similarities of compound **2**c with ACh, Ch and edrophonium have been marked by bold lines.

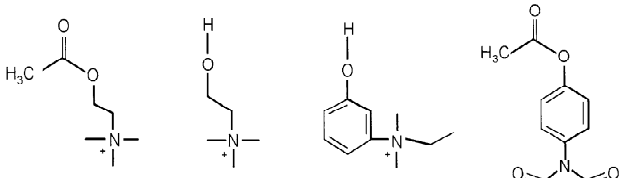

Although it has been demonstrated by several studies that molecules with a positive charged ammonium group like edrophonium and ACh are more selectively bound to the enzyme than analogous uncharged molecules (Harel et al., 1993), some of the compounds that we prepared are neutral molecules (**2** and **4**) in order to enhance the lipophilicity of the inhibitors. Nevertheless, the imide group in compounds **2** and **4** is polarizable and the electron density of the free electron pair of the nitrogen atom is delocalized through the carbonyl groups and aromatic ring. Thus, more than two mesomeric structures with partial positive charges on the nitrogen atom can be formulated, a fact that may be important for the recognition between the inhibitor and the Ch subsite of AChE.

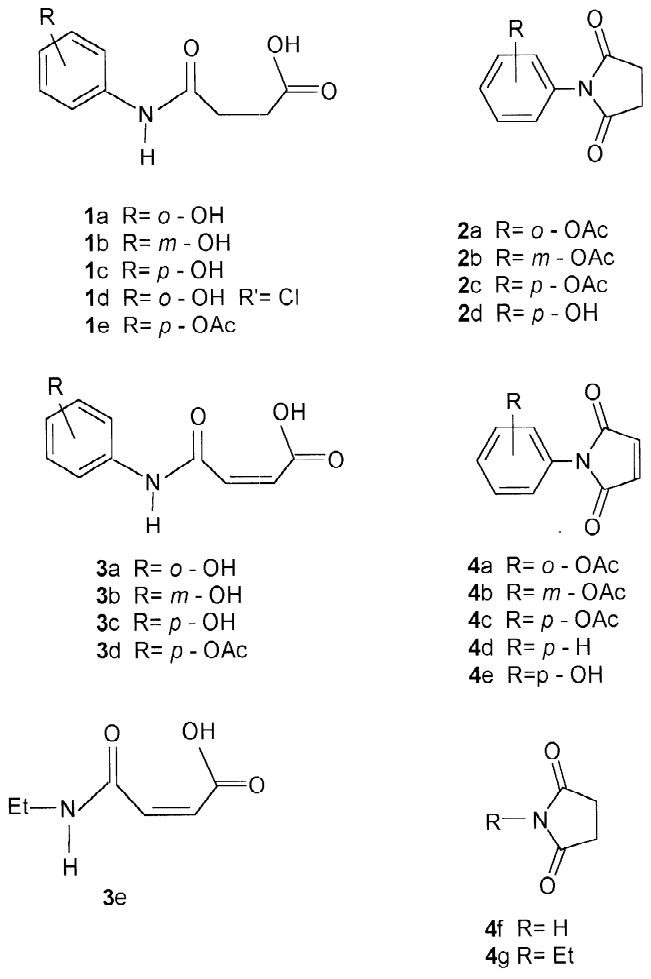

Fig. 1. Structures of the derivatives of succinic (**1**–**2**) and maleic acids (**3**–**4**) that have been examined as reversible and irreversible inhibitors of AChE in this work.

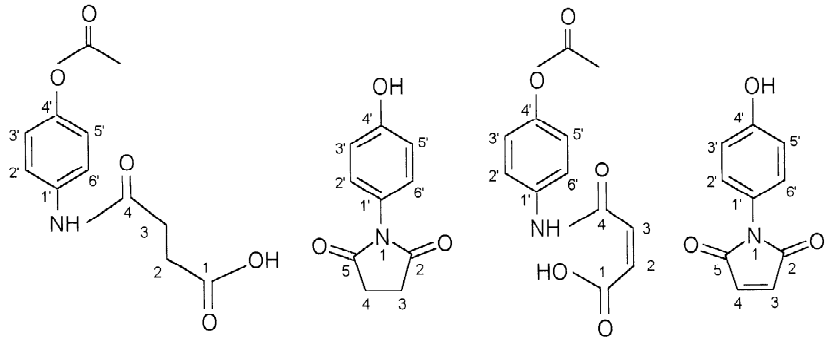

1e 2d 3d 4e

Fig. 2. Structures of the new compounds **1**e, **2**d, **3**d and **4**e.

There is another important feature during the design of molecules **1**–**4**, it was considered that succinic amides/imides (**1**–**2**) and maleic amides/imides (**3**–**4**) may react in different ways with bionucleophiles such as thiols and imidazoles. Both succinic amides and imides are susceptible to 1,2-addition reactions at the carbonyl functions (Groutas et al., 1995); however, maleic amides and imides are susceptible to 1,2-addition, and at the same time to 1,4-addition reactions at the α,β-unsaturated carbonyl function, especially with thiols and imidazole derivatives (Walker, 1994). Therefore, it could be expected that the unsaturated compounds **3**a–d and **4**a–g react as irreversible inhibitors, while compounds **1**a–e and **2**a–d without the C=C double bond could react as reversible inhibitors.

To our knowledge, the following study is the first report dealing with the AChE inhibitory activity of these types of compounds.

2. Materials and methods

2.1. Synthesis

The synthesis of amides and imides **1**–**4** was achieved by slight modifications of a previously reported method (Sauers, 1969; Walker, 1994; Trujillo-Ferrara et al., 1999), which briefly consists of the following.

Reaction of maleic or succinic anhydride with the appropriate arylamide in the presence of anhydrous tetrahydrofuran at room temperature generated the corresponding amides (**1**a–c) or vinyl amides (**3**a–c) in nearly quantitative yields (94–98%). The starting materials were subsequently transformed to the corresponding imides (**2**a–c and **4**a–c) by heating them in acetic anhydride with an equimolecular amount of sodium acetate.

All synthesized and assayed compounds were characterized by ^{1}H and ^{13}C nuclear magnetic resonance (NMR) and infrared spectra (IR). ^{1}H and ^{13}C NMR spectra were compared to our recently reported data on these molecules (Trujillo-Ferrara et al., 1999). ^{1}H and ^{13}C NMR spectra were recorded on a Joel GSX-270 spectrometer. Approximately 10% sample solutions in DMSO-d_6 were prepared in 5-mm tubes with samples referred to tetramethylsilane. Chemical shifts are stated in ppm and the coupling constants in Hz; they are positive, when the signal is shifted to higher frequencies than the standard. Infrared spectra were measured with a MIDAC M2000 FT-IR spectrophotometer from KBr pellets. Melting points were determined in open ended capillary tubes in an Electrothermal 9300 digital apparatus and are uncorrected.

2.1.1. Synthesis of 4-(4′-acetoxy-phenylamino)-4-oxo propanoic acid *1*e (Fig. 2)

A solution of 4-(4′-hydroxy-phenylamino)-4-oxo propanoic acid **1**c (3 g, 14.4 mmol) in the presence of anhydrous tetrahydrofuran (60 ml), pyridine (50 μl) and an excess of acetic anhydride (60 ml) was heated and stirred at 60 °C for 5 h, followed by evaporation of the solvent under vacuum. The residue was washed three times with 0.001 M HCl, yielding **1**e (2.7 g, 90%). Melting point of **1**e 260–262 °C; ^{1}H NMR (DMSO-d_6, 270 MHz) δ (ppm), 2.50 (1H, t, $J=6$, H-2), 2.52 (1H, t, $J=6$, H-3), 7.00 (2H, d, $J=9$, H-2′,6′), 6.76 (2H, d, $J=9$, H-3′,5′); ^{13}C NMR (67.5 MHz) δ (ppm), 170.00 (C-1), 128.40 (C-2′,6′), 115.40 (C-3′,5′); IR (KBr) ν (cm^{-1}) 3264 (OH, carboxylic acid), 1686 (C=0), 1204 (C–N), 1189 (C–H).

2.1.2. Synthesis of 1H-(4′-hydroxy-phenyl)-2,5-pyrrolidine dione *2*d (Fig. 2)

A solution of 4-(4′-hydroxy-phenylamino)-4-oxo propanoic acid **1**c (3 g, 14.4 mmol) in the presence of anhydrous tetrahydrofuran (60 ml) and equimolecular amount of sodium acetate (1.14 g) and acetic anhydride (1.5 ml) was heated and stirred at 60 °C for 8 h, followed by evaporation of the solvent under vacuum. The residue was washed three times with 0.001 M HCl, yielding **2**d (2.8 g, 95%). Melting point of **2**d >300 °C; ^{1}H NMR (DMSO-d_6, 270 MHz) δ (ppm), 2.73 (4H, s, H-3), 7.01 (2H, d, $J=8.6$, H-2′,6′), 6.82 (2H, d, $J=8.6$, H-3′,5′);

^{13}C NMR (67.5 MHz) δ (ppm), 177.76 (C-1), 28.87 (C-2, C-5), 157.65 (C-4′), 128.83 (C-2′,6′), 135.84 (C-3′,5′). IR (KBr) ν (cm^{-1}), 3268 (OH), 1720 (C=O), 1686 (C=O).

2.1.3. Synthesis of 4-(4′-acetyloxyphenylamino)-4-oxobut-Z-2-enoic acid 3d (Fig. 2)

A solution of 4-(4′-hydroxy-phenylamino)-4-oxobut-*Z*-2-enoic acid **3**c (3 g, 14.5 mmol) in the presence of anhydrous tetrahydrofuran (60 ml), pyridine (50 μl) and an excess of acetic anhydride (60 ml) was heated and stirred at 60 °C for 8 h, followed by evaporation of the solvent under vacuum. The residue was washed three times with 0.001 M HCl, yielding **3**d (2.7 g, 90%). Melting point of **3**d 186–188 °C. ^{1}H NMR (DMSO-d_6, 270 MHz) δ (ppm), 6.48 (1H, s, J=12, H-2), 6.60 (1H, s, J=12, H-3), 6.80 (2H, d, J=9, H-2′,6′), 7.43 (2H, d, J=9, H-3′,5′); ^{13}C NMR (67.5 MHz) δ (ppm), 167.00 (C-1), 131.00 (C-2), 130.00 (C-3), 160.30 (C-4), 121.20 (C-2′,6′), 113.00 (C-3′,5′). IR (KBr) ν (cm^{-1}), 3334 (OH, carboxylic acid), 1728 (C=0), 1233 (C–N), 1193 (C–H).

2.1.4. Synthesis of 1H-pyrrole-1-(4′-hydroxyphenyl)-2,5-dione 4e (Fig. 2)

A solution of 4-(4′-hydroxy-phenylamino)-4-oxobut-*Z*-2-enoic acid **3**c (3 g, 14.4 mmol) in the presence of anhydrous tetrahydrofuran (60 ml) and equimolecular amount of sodium acetate (1.14 g) and acetic anhydride (1.5 ml) was heated and stirred at 60 °C for 8 h, followed by evaporation of the solvent under vacuum. The residue was washed three times with 0.001 M HCl, yielding **4**e (2.5 g, 83.3%). Melting point **4**e 185–187 °C. ^{1}H NMR (DMSO-d_6, 270 MHz) δ (ppm), 7.10 (1H, s, H-3), 6.82 (1H, d, J=8.8, H-3′5′), 7.07 (1H, d, J=8.8, H-2′,6′); ^{13}C NMR (67.5 MHz) δ (ppm) 171.19 (C-3, C-4), 135.39 (C-2), 123.30 (C-1′), 157.88 (C-4′), 129.28 (C-2′,6′), 116.25 (C-3′,5′). IR (KBr) ν (cm^{-1}), 3485 (OH), 1703 (C=O).

In order to confirm the stability of phenyl acetates, the reaction of the compounds **2**c and **4**c in the buffer and enzyme solution was tested at pH 8 and 37 °C for 24 h and the reaction was followed by thin layer chromatography; the starting material and the hydrolysis products were not observed. The hydrolysis was undertaken in ETOH/H_2O pH 1 at 50 °C and only in these conditions was the acetate group lost. The hydrolysis products were characterized by ^{1}H and ^{13}C NMR spectra.

2.2. X-ray crystallography

X-ray diffraction studies of single crystals were realized on an Enraf-Nonius CAD4 diffractometer ($\lambda_{\mathrm{Mo\ K\alpha}}$= 0.71069 Å, monochromator: graphite, T=293 K, ω–2θ scan). Cell parameters were determined by least squares refinement on diffractometer angles for 24 automatically centered reflections. Absorption correction was not necessary; corrections were made for Lorentz and polarization effects. Direct methods (SHELXS-86) were used for structure solution and the CRYSTALS (version 9, 1994) software package for refinement and data output. Non hydrogen atoms were refined anisotropically. Hydrogen atoms were determined by differences in the Fourier maps, and one overall isotropic thermal parameter as well as their coordinates were refined. $I > 3\sigma(I)$ ($R = \Sigma(\|F_o| - |F_c\|)/\Sigma|F_o|$, $R_w = [\Sigma w(|F_o| - |F_c|)^2/\Sigma wF_o^2]^{1/2}$. In all cases only independent reflections on the basis of Friedel's law have been collected and a reflection–parameter ratio >5 has been considered sufficient for the type of structural studies performed here. The asymmetric unit of compounds **1**c, **2**a and **2**b contains two independent molecules.

The most important crystallographic data have been summarized in Table 1. Lists with atomic parameters, bond lengths, bond angles and thermal parameters have been deposited at the Cambridge Crystallographic Data Center.

2.3. Enzyme kinetics

For all in vitro kinetic experiments true bovine erythrocyte AChE (EC 3.1.1.7), type XII from Sigma, with a specific activity of hydrolysis of 1.0 μmol/min per mg of protein in 0.10 M phosphate buffer at pH 8.0 and T=37 °C were used. Acetylcholine iodide from Sigma was used as a substrate at various concentrations both below and above but near K_m in a phosphate buffer at pH 8. The inhibitors were dissolved in ethanol (3% v/v) and immediately diluted to the desired working concentration with the same phosphate buffer used for the preparation of the AChE suspension.

The enzymatic inhibition measurements of the different inhibitors were carried out in the presence and absence of a fixed concentration of inhibitors and at different substrate concentrations.

For the dialysis kinetic studies, a solution of enzyme (0.04 ml, 0.5 M) and fixed inhibitor concentration (1.2 ml) was prepared and dialyzed against 100 ml buffer at 37 °C for 2 h using regenerated cellulose dialysis membranes SPECTRAPOR®. Aliquots of 0.08 ml of the enzyme–inhibitor mixture were taken in time intervals of 0, 20, 40, 60, 90, 120 min and added to 0.12 ml of substrate (2.85×10^{-4} M), and after an hour of incubation the enzyme activity was measured. A control solution prepared with enzyme (0.04 ml) and buffer (1.2 ml) was treated similarly.

For the time–concentration-dependence kinetic, test and control solutions were prepared as before, but without dialysis, and the enzyme activity was measured in the same time intervals.

At the end of incubation, the concentration of the remaining ACh was detected by a modified version of the colorimetric method of Bonting and Featherstone (1956). Therefore, 0.08-ml aliquots were transferred under rapid

Table 1
Crystallographic data for compounds **1**d, **2**a–c and **3**a

Crystal data	**1**d[a]	**2**[a]	**2**b[a]	**2**c	**3**[a]
Formula	$C_{10}H_{10}ClNO_4$	$C_{12}H_{11}NO_4$	$C_{12}H_{11}NO_4$	$C_{12}H_{11}NO_4$	$C_{10}H_9NO_4$
Crystal size (mm)	0.5×0.6×0.6	0.3×0.5×0.5	0.4×0.5×0.6	0.2×0.2×0.4	0.3×0.3×0.3
M_w (g mol^{-1})	243.64	233.22	233.22	233.22	207.19
Space group	*P*-1	*Pcab*	$P2_1/a$	$P2_1$	$P2_12_12_1$
Cell parameters					
a (Å)	14.302(1)	9.686(1)	12.199(1)	7.827(2)	6.793(1)
b (Å)	5.344(1)	12.318(4)	12.017(1)	6.250(2)	10.682(1)
c (Å)	14.322(1)	19.072(9)	16.291(1)	12.068(4)	12.853(1)
α (°)	90.23 (1)	90	90	90	90
β (°)	101.22(1)	90	110.69(1)	106.34(3)	90
γ (°)	89.79(1)	90	90	90	90
V (Å^3)	1073.77(1)	2275.5(9)	2234.2(3)	566.5(3)	932.6(1)
Z	4	8	8	2	4
μ (mm^{-1})	0.350	0.097	0.099	0.097	0.108
ρ_{calcd} (g cm^{-3})	1.51	1.36	1.39	1.37	1.48
Data collection					
No. collected refl.	3436	2834	5957	1558	1211
No. ind. refl.	3294	2477	4841	1490	1127
No. observed refl.	2500	1576	3531	971	955
Refinement					
R	0.045	0.037	0.038	0.031	0.039
R_w	0.045	0.032	0.032	0.024	0.044
W	$1/\sigma^2$	$1/\sigma^2$	$1/\sigma^2$	$1/\sigma^2$	$1/\sigma^2$
No. of variables	351	189	375	189	165
GOOF	2.73	2.63	1.85	1.99	1.97

[a] Two independent molecules in the asymmetric unit.

stirring to a 3.0-ml cuvette of 1.0 cm pathlength with 2.0 ml of ferric chloride (0.086 mmol) and hydroxyl amine (0.47 mmol). As a colorimetric blank, a cuvette with exactly the same components including the inhibitor but no ACh was prepared. Absorption measurements were realized at $\lambda = 540$ nm, both with a control and a test sample. The extinction of the test sample was subtracted from the value obtained for the blank. Data are quoted as mean value of three experiments, which varied by less than 8% in relation to each other.

In the case of the irreversible inhibitors, competitive experiments with edrophonium (3-hydroxyphenyl-ethyldimethylammonium iodide), a well-known reversible inhibitor, were also carried out. The competitive inhibitor was added to the enzyme–substrate mixture just before the inhibitor under study.

3. Results and discussion

All compounds were characterized by ^{1}H and ^{13}C NMR spectroscopy in order to verify their purity, and the data were compared with the reported values (Trujillo-Ferrara et al., 1999; Hargreaves et al., 1970). In the case of the new compounds **1**e, **2**d, **3**d and **4**e all the aromatic moieties showed an AA′BB′ system and $J = 8.7$ Hz. For the non-aromatic moiety of the new compounds the results were as follows: **1**e, H-2 and H-3 protons appear as triplets, the downfield triplet arising from the H-3 and the highfield triplet from the H-2. The magnitude of coupling constant is found to be identical between H-2 and H-3 (6 Hz). In case of **2**d its formation was confirmed by the disappearance of the characteristic triplets of **1**c and generation of the A_4 system. For **3**d the assignment of H-2 and H-3 in the vinylic moiety was achieved by COLOC experiments which exhibit an AB system with a $J = 12$ Hz and the signals of vinylic carbons were assigned unambiguously by ^{1}H-^{13}C HETCOR. **4**e is the cyclical product derived from **3**c in which the AB vinylic system is transformed to an A_2 system and that absorbs at 7.12 ppm.

Due to the difference in reactivity between ligands **1**–**2** and the α,β-unsaturated ligands **3**–**4**, two different kinetic models had to be considered for the inhibition. Compounds **1**a–e and **2**a–d behaved as competitive reversible inhibitors and their inhibitory kinetics were evaluated by the Lineweaver and Burk (1934) method; different substrate concentrations above and below the Michaelis constant K_m of AChE for ACh were assayed. The inhibitor concentration was always kept close to one which corresponds to 50% inhibition of the enzyme activity (IC_{50}). Straight lines were obtained in the case of compounds **1**b–c and **2**b–c (Fig. 3), whereas for compounds **1**a and **2**a (*ortho* derivatives) the inhibition was not observed even at concentrations as high as 10 μM. For the active compounds, the existence of a covalent bond between inhibitor and enzyme could be excluded, because the enzyme activity could be recovered by dialysis within 2 h. In the case of these reversible inhibitors, V_{max} did not change at high substrate

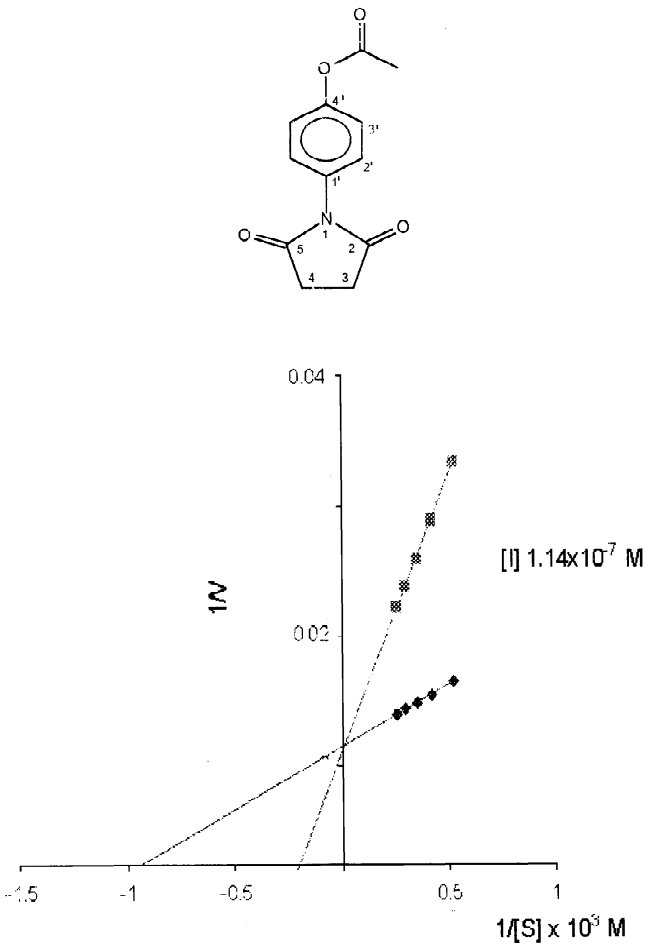

Fig. 3. Lineweaver–Burk plot of in vitro acetylcholinesterase inhibition by 1H-pyrrolidine-1-(3′-acetyloxyphenyl)-2,5-dione (**2**c). Each point represents the mean value of three determinations, which varied by less than 6% in relation to it.

concentration, indicating that inhibition is competitive. The inhibitory effects of the two families of compounds on AChE were compared among themselves and then with several known reversible inhibitors, as shown in Table 2. The inhibitory activity of the *meta*-substituted aminophenol derivatives **1**b and **2**b was lower than that of the *para*-substituted derivatives. The most potent inhibitor among this class of compounds was succinimide **2**c with $K_i = 7.8 \times 10^{-8}$ mol/l. It is therefore more active than edrophonium, physostigmine (Gregor et al., 1992) and, however, it approximately presents eight times less activity than tacrine, $K_i = 1 \times 10^{-8}$ mol/l, and 27 times less activity than E2020, $K_i = 3 \times 10^{-9}$ mol/l (Kawakami et al., 1996).

In contrast, aminophenol derivatives with vinylic moiety **3**b–d and **4**b–e behaved as irreversible inhibitors since they met the three criteria of Abeles and Maycock (1976) for irreversible inhibition. The most definitive way of testing irreversible inhibition requires the complete characterization of the enzyme–inhibitor adduct. Such investigation is time-consuming and frequently very difficult to do because of the limited amounts of enzyme which are generally available. However, relatively simple kinetic experiments can give reasonable assurance that our proposed inhibitors were acting in a covalent form when the following conditions were met: (a) time dependence provides good but not definitive evidence that covalent modification had taken place and the demonstration that the loss of enzyme activity at a constant inhibitor concentration was of the first order provided evidence that inactivation occurred before the inhibitor was released from the enzyme; (b) the rate of inhibition should have been proportional to the inhibitor concentration at low concentrations of the same; (c) the rate of inactivation at a given inhibitor concentration should have diminished as

Table 2
Kinetic data for reversible and irreversible inhibition on acetylcholinesterase by aminophenol derivatives of succinic and maleic acid

Compound	Type of inhibition	K_i (M)	k_{+2} (10^{-2} s^{-1})	k_i (10^4 M^{-1} s^{-1})
1b	Reversible	46.0±0.3		
1c	Reversible	1.3±0.5		
1e	Reversible	6.6±0.3		
2b	Reversible	40.0±0.3		
2c	Reversible	0.005±0.4		
2d	Reversible	28.5±0.4		
3b	Irreversible	2.3±1.2	0.013±0.02	0.0056±0.0001
3c	Irreversible	1.2±1.3	6.0±0.4	5.0±0.3
3d	Irreversible	0.8±0.5	3.0±0.8	3.8±1.0
4b	Irreversible	Unstable	Unstable	Unstable
4c	Irreversible	0.54±0.2	1.0±0.3	1.85±1.0
4d	Irreversible	2.7±1.5	3.0±2.3	1.1±0.1
4e	Irreversible	1.8±1.0	2.0±0.8	1.1±0.8
Edrofonio[a]	Reversible	18.5		
Neostigmina[a]	Reversible	14.4		
Tacrine[a]	Reversible	0.01		
E2020	Reversible	0.003		

[a] Kinetic data on bovine erythrocyte AChE, type XII from Sigma.

the substrate or competitive reversible inhibitor concentration increased. These two kinetic phenomena, saturation kinetic and substrate or competitive inhibitor protection against inhibition, are necessary consequences of the involvement of the enzyme's active site in the inhibition process for the aforementioned. The inhibitory kinetics of the compounds **3**b–d and **4**c–e were evaluated by the method established by Kitz and Wilson (1962) and they all met these conditions and therefore it may be suggested that they are active site-directed irreversible inhibitors, because after exposure to edrophonium (a reversible inhibitor which binds at the Ch subsite) and then dialysis, the enzyme recovered its activity.

For this reason, the following reaction sequence between the enzyme and the inhibitor was considered for these types of compounds

$$E + I \underset{k_{-1}}{\overset{k_{+1}}{\rightleftharpoons}} EI \underset{k_{-2}}{\overset{k_{+2}}{\rightleftharpoons}} EI'$$

whereby EI is a reversible enzyme–inhibitor complex and EI′ an irreversible one. The existence of an irreversible complex was proved by exhaustive dialysis of the enzyme–substrate complex after inhibition and later measurement of the enzyme activity, the result of which was that it could not be recovered. Therefore k_{+2} must be very small. The kinetics of the enzyme inhibition were evaluated by Eqs. (1) and (2) (Kitz and Wilson, 1962)

$$\text{In} = \frac{[E]}{[E_T]} = -\frac{k_{+2}t}{1 + K_1[I]^{-1}} \quad \begin{matrix}\text{with } [E_T] = [E] + [EI'] \\ \text{and } [E] = [E] + [EI]\end{matrix} \qquad (1)$$

$$\frac{1}{k_{app}} = \frac{1}{k_{+2}} + \frac{K_1}{k_{+2}} = \frac{1}{[I]} \quad \text{with } k_{app} = \frac{k_{+2}}{1 + K_1[I]^{-1}}. \qquad (2)$$

The kinetic data obtained were plotted according to Eq. (1). From Fig. 4 (plot A) the concentration and time dependence of the irreversible inhibition of compound **4**c can be seen. The kinetic of the inhibition of AChE is of first order as evidenced by a plot of the inverse of k_{app} versus the inverse of the inhibitor concentration [I]. Eq. (2) is the equation of a straight-line graph. As in the case of the *ortho* derivatives, **1**a and **2**a, **3**a and **4**a did not cause any inhibition at 10 μM, even after 1 day of contact with the enzyme. The same behavior was observed with compounds **3**e and **4**f–g.

In Fig. 4 (plot B) the linear plot of compound **4**c according to Eq. (2) is shown and a reasonable correlation was obtained. The regression line did not pass through the origin, but intercepted the positive *y*-axis, a fact which indicates that initially reversible enzyme–inhibitory complexes were formed (Kitz and Wilson, 1962). The rate constants for the inhibitory activity k_{+2} and the equilibrium constants for the enzyme inhibition K_i of the α,β-unsaturated compounds **3**b–d and **4**c–e are listed in Table 2. As in the case of the above studied reversible inhibitors, *meta*-substituted maleamide and maleimide derivatives were less potent than *para*-substituted ones. The most potent inhibitor was maleimide **4**c with values of $k_{+2} = 1.0 \times 10^{-2}$ s^{-1} and $K_i = 5.4 \times 10^{-7}$ mol/l. Therefore **4**c is more active than neostigmine (Jaen and Moos, 1992), diisopropylfluorophosphate and paraoxon, but less active than tacrine, 1×10^{-8} M, and E2020, 3×10^{-9} M (Boyd et al., 2000). Compounds **4**d and **4**e had a significantly lower activity than **4**c, so the presence of an acetyl group in the aromatic *para* position increased recognition; compounds **3**e and **4**f–g that have neither aromatic rings nor acetyl groups were clearly inactive. The importance of the aromatic ring in active compounds is shown by the results of **3**e and **4**f–g which have alkyl substituents instead of an aromatic ring and which did not inhibit the enzyme even at a concentration of 10 μM.

The inhibition of AChE by maleic acid aminophenol derivatives was lower with edrophonium than without it, as would be expected in the event that the active site is involved in the inhibition. With this observation it is possible to conclude that all active irreversible molecules found in this study block the active site of AChE, particularly the choline subsite. Also it can be proposed that the first step for both types of inhibitors is the formation of a reversible enzyme–inhibitor complex with the α,β-unsaturated derivatives **3**b–d and **4**c–e; this reversible enzyme–inhibitor complex by addition reactions with nucleophilic substituents of the enzyme, or a π–π recognition of high affinity is possible in an irreversible interaction.

The X-ray structure of AChE has established the existence of Trp84. In addition, the active site contains imidazole groups, which are known to undergo nucleophilic addition reactions with α,β-unsaturated carbonyl derivatives. Firstly, there are imidazol residues in the catalytic triad (His440) and at the gorge rim (His287) (Sussman et al., 1991). Additionally, there are two Tyr residues, one at the bottom and the other one half way up the gorge of the active site. So the reaction between imidazol and α,β-unsaturated derivatives is possible (Fig. 5).

In order to support this hypothesis we reacted histidine with compound **4**c in H_2O/EtOH (1:1) and clearly a 1,2-addition product was observed and characterized by ^{1}H and ^{13}C NMR spectroscopy, showing that the vinylic protons that absorbed at 7.2 ppm disappeared and in their place appeared an AB system at 6.3 and 6.5 ppm with $J = 12$ Hz; also the imide carbonyl carbon disappeared and the amide carbonyl at 164 ppm appeared which are typical values of chemical shifts for amide carbonyls.

In order to obtain more information about the type of interaction between the inhibitors and the active site of AChE, the molecular structures of compounds **2**a–c (Fig. 6) were determined by X-ray crystallography. The structures of these compounds are outlined together with the structure of the *trans,trans* conformer of ACh, which has been found to be the most adequate conformation of the complex with AChE (Canepa et al., 1966).

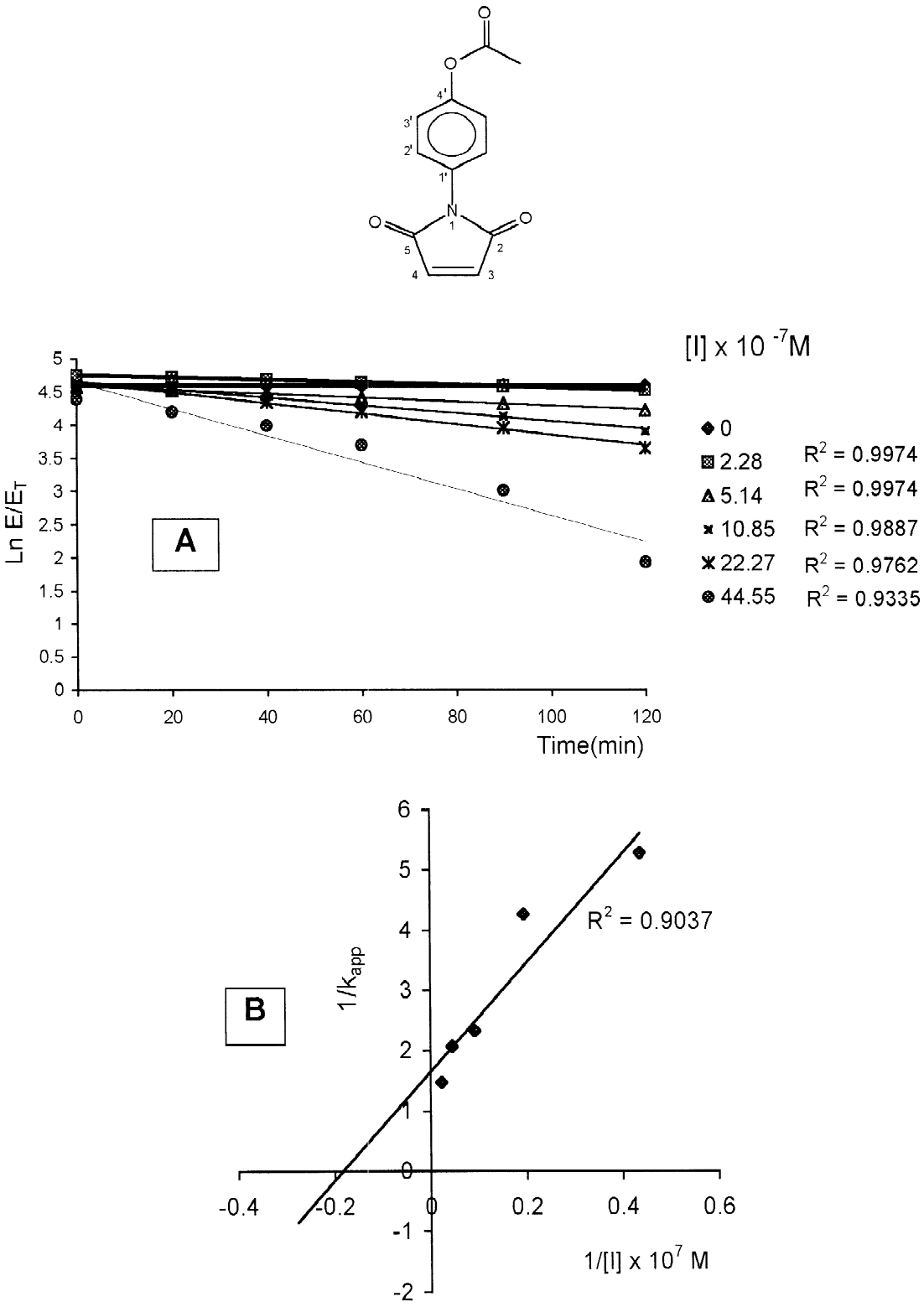

Fig. 4. Time- and concentration-dependent inhibition of acetylcholinesterase by 1H-pyrrole-1-(4′-acetyloxyphenyl)-2,5-dione (**4**c). Plot A shows how the concentration of the enzyme–inhibitor complex [EI] decreases with enhanced incubation time. Plot B shows that the inhibition kinetics is of first order. The line corresponds to the best fit by linear regression. All points are the mean values of three determinations.

The length and width of molecules **1**d and **3**a are listed in Table 3 in comparison to the corresponding data of *trans,trans*-ACh and compounds **2**a–c.

An analysis of the molecular structures of compounds **2**a–c shows that both the acetyl group and the succinimide function are twisted out of the molecular plane of the

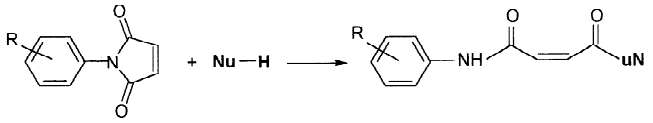

Fig. 5. Possible mechanisms for the formation of a covalent bond between enzyme and inhibitor molecules **3** and **4**. Nu-H is acetylcholinesterase with one of its nucleophilic imidazole groups.

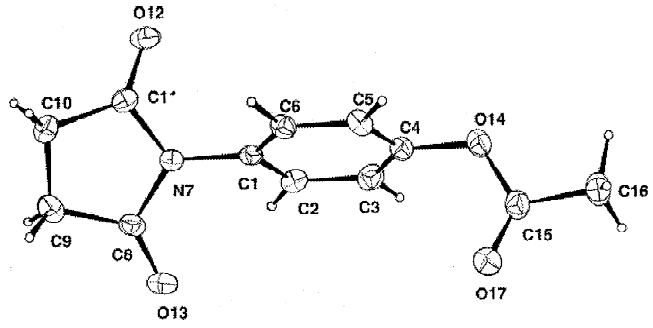

Fig. 6. Molecular structure of **2**c by X-ray crystallography.

phenyl ring. Although compound **2**a is the compound with the highest structural similarity to ACh, this molecule has been found to be inactive as an inhibitor. One reason may be its large and compact molecular structure with a length of 7.9 Å and a width of 7.3 Å that may inhibit diffusion through the gorge to the active site. The gorge has a width of 4.5 Å at its narrowest point. Although compound **2**b is as broad as **2**a, diffusion through the gorge may be easier for this molecule because the acetyl and succinimide groups are more separated (at the *ortho* position, O–N 2.78 Å; and at the *meta* position, O–N 4.84 Å). The *para*-substituted derivative **2**c with a width of only 4.5 Å and a distance O–N of 5.78 Å should pass through the gorge more easily and this may be the reason why this molecule has been found to be an $\sim 10^3$ more potent reversible inhibitor than compound **2**b. In the same context as the aforementioned, with compounds **4**, the *para*-substituted aminophenol derivative of maleamic acid **4**c is also thinner than **4**b, a fact that might explain the higher activity of the *para*-substituted derivative. The *ortho*-substituted aminophenol derivatives **1**a and **3**a are also small molecules and at first sight it may be surprising that they are inactive. A possible explanation might be related to the presence of a polar hydroxyl group at the lateral site of the molecules that reduces its lipophilicity. This reduced lipophilicity at the lateral site of the molecule may inhibit the passage of the compound through the highly hydrophobic gorge of the enzyme to the active site.

Table 3
Comparison of some important structural data between *trans,trans*-ACh, **1**a, **2**a–c and **3**a. Only atom to atom distances have been considered. The structural data of compound **1**a have been estimated on the basis of the molecular structure of **1**d

Compound	Length of the molecule (Å)	Width of the molecule (Å)	O12/O13 ··· O17 distance (Å)
trans,trans-ACh	8.7	3.9	–
1a	9.0	5.3	–
3a	10.4	5.5	–
2a	7.9	7.3	3.50/6.34
2b	9.4	7.3	4.22/7.07
2c	10.9	4.5	5.95/7.45

Another explanation for the inactivity of the *ortho*-substituted derivatives of compounds **1**a and **3**a could be the observation that these molecules have a close structural relationship to the *gauche* conformation of ACh. It has been demonstrated that the *gauche* conformation of ACh is probably inactive at the catalytic site of AChE, although it is the most stable conformation of ACh (Canepa et al., 1966). The inactivity results from a sterical inhibition in the formation of the tetrahedral intermediate generated during the acylation in the hydrolysis of ACh by AChE (Harel et al., 1996; Silman et al., 1992).

In contrast, the structures of the *para*-substituted derivatives of **2**c and **4**c are more related to the *anti*-conformation of ACh, the conformer with the most adequate structure for comparison in the catalytic triad prior to hydrolysis.

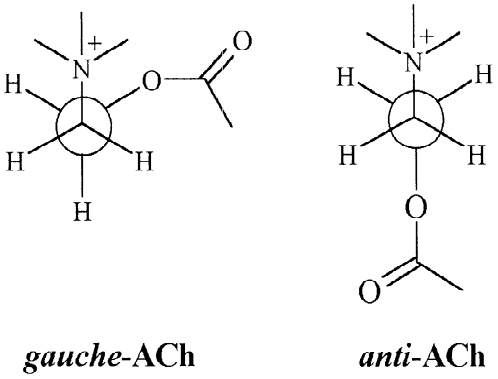

***gauche*-ACh** ***anti*-ACh**

A further result of the present study is the observation that the molecular dimensions, as well as the presence of an aromatic ring system and the polarity of functional groups at the hydrophobic part of the molecules used as inhibitors must be important factors for their inhibitory activities and that the non-aromatic imide molecule is not active as an inhibitor at all.

The conclusions of this study can be summarized as follows for both families: (a) the aromatic moiety plays a critical role in the recognition of the active site; (b) in case of the reversible inhibitor, when the ester function took the place of the hydroxyl fragment, there was an important increase in the affinity; (c) the distance between phenolic hydroxyl and nitrogen was critical because the inhibition is *ortho* ≪ *meta* < *para*. These conclusions are in agreement with a recent comparative QSAR analysis of AChE inhibitors currently being studied for the treatment Alzheimer's disease (Recatini et al., 1997).

Finally, further studies are important in order to modify

the functional groups at the aromatic ring and the succinamic, maleamic, succinamic and imide moiety, respectively, in order to enhance their inhibitory activity still further.

Acknowledgements

The authors wish to thank Arturo Bustamante Quezada for technical assistance and CONACYT and SEGEPI for financial support.

References

Abeles, R.H., Maycock, A.L., 1976. Suicide enzyme inactivators. Acc. Chem. Res. 9, 313–319.

Baker, B.R., Alumaula, P.J., 1963. Non classical enzyme inhibitors. Pharm. Sci. 52, 914–915.

Berman, H.A., Leonard, K., 1991. Interaction of tetrahydroaminoacridine with acetylcholinesterase and butyrylcholinesterase. Mol. Pharmacol. 41, 412–418.

Bonting, S.L., Featherstone, R.M., 1956. Ultramicro assay of the cholinesterase. Arch. Biochem. Biophys. 61, 89–98.

Bourne, Y., Marchot, P., Taylor, P., 1995. Acetylcholinesterase inhibition by fasciculin: crystal structure of the complex. Cell 83, 493–506.

Boyd, A.A., Marnett, A.B.L. et al., 2000. Probing the active center gorge of acetylcholinesterase by fluorophores linked to substituted cysteines. J. Biol. Chem. 275, 22401–22405.

Canepa, F.G. et al., 1966. Structure of acetylcholine and other substrates of cholinergic systems. Nature 210, 907–909.

Gregor, V.E., Emmering, M.R., Lee, C., Moore, J.C., 1992. The synthesis and in vitro acetylcholinesterase and butyrylcholinesterase inhibitor activity of tacrine derivatives. Bioorg. Med. Chem. Lett. 2, 861–867.

Grisaru, D., Sternfeld, M., Eldor, A., Glick, D., Soreq, H., 1999. Structural roles of acetylcholinesterase variants in biology and pathology. Eur. J. Biochem. 264, 672–686.

Groutas, W.C., Brubaker, M.J., Chong, L.S., Venkataraman, R., Huang, H., Eppo, J.B., Kuang, R., Hoidan, R.G., 1995. Design, synthesis and biological evaluation of succinimide derivatives as potential mechanism-based inhibitors of human leukocyte elastase, cathepsin G and proteinase 3. Bioorg. Med. Chem. 3, 375–381.

Harel, M., Quinn, D.M., Nair, H.K., Silman, I., Sussman, J.L., 1996. The X-ray structure of a transition state analog complex reveals the molecular origins of the catalytic power and substrate specificity of acetylcholinesterase. J. Am. Chem. Soc. 118, 2340–2346.

Harel, M., Schalk, I., Sabatier, L.E., Bouet, F., Goeldner, M., Hirth, C., Axelsen, P.H., Silman, I., Sussman, J.L., 1993. Quaternary ligand binding to aromatic residues in the active-site gorge of acetylcholinesterase. Proc. Natl. Acad. Sci. USA 90, 9031–9035.

Hargreaves, M.K., Pritchard, J.G., Dave, A.R., 1970. Cyclic carboxylic monoimides. Chem. Rev. 70, 439.

Jaen, J.C., Moos, W.H., 1992. Cholinomimetics and Alzheimer's disease. Bioorg. Med. Chem. Lett. 2, 777–780.

Kawakami, Y., Inoue, A., Kawai, T., Wakita, M., Sugimoto, H., Hopfinger, A.J., 1996. The rationale for E2020 as a potent acetylcholinesterase inhibitor. J. Bioorg. Med. Chem. 4, 1419–1426.

Kitz, R., Wilson, I.B., 1962. Esters of methanesulfonic acid as irreversible inhibitors of acetylcholinesterase. J. Biol. Chem. 237, 3245–3249.

Kryger, G., Silman, I., Sussman, J.L., 1999. Structure of acetylcholinesterase complexed with E2020 (Aricept®): implications for the design of new anti-Alzheimer drugs. Structure 7, 297–307.

Lin, G., Lai, C., Liao, W., 1999. Molecular recognition by acetylcholinesterase at the peripheral anionic site: structure–activity relationships for inhibitions by aryl carbamates. Bioorg. Med. Chem. 7, 2683–2689.

Lineweaver, H., Burk, D., 1934. The determination of enzyme dissociation constants. J. Am. Chem. Soc. 56, 658–666.

Quinn, D.M., 1987. Acetylcholinesterase: enzyme structure, reaction dynamics, and virtual transition states. Chem. Rev. 87, 955–979.

Recatini, M., Cavalli, A., Hansch, C., 1997. A comparative QSAR analysis of acetylcholinesterase inhibitors currently studied for the treatment of Alzheimer's disease. Chem. Biol. Interact. 105, 199–228.

Sauers, C., 1969. The dehydratation of N-arylmaleamic acid with acetic anhydride. J. Org. Chem. 34, 2275–2279.

Schumacher, M., Camp, S., Maulet, Y., Newton, M., MacPhee-Quigley, K., Taylor, S., Friedmann, T., Taylor, P., 1986. Primary structure of *Torpedo californica* acetylcholinesterase deduced from its cDNA sequence. Nature 319, 407–409.

Silman, I., Krejci, E., Duval, N., Bon, S., Chenal, P., Harel, M., Sussman, J.L., Massoulie, J., 1992. In: Shafferman, A., Velan, B. (Eds.), Multidisciplinary Approach to Cholinesterase Functions.

Sussman, J.L., Harel, M., Frolow, F., Oefner, C., Goldman, A., Toker, L., Silman, I., 1991. Atomic structure of acetylcholinesterase from *Torpedo californica*: a prototypic acetylcholine-binding protein. Science 253, 872–879.

Taylor, P., 2001. In: Hardman, J., Limbird, L. (Eds.), Anticholinesterase Agents In The Pharmacological Basis of Therapeutics. McGraw Hill, New York.

Taylor, P., 1998. Development of acetylcholinesterase inhibitors in the therapy of Alzheimer's disease. Neurology 51 (Suppl. 1), S30–S35.

Trujillo-Ferrara, J., Santillan, R., Beltrán, H.I., Farfán, N., Höpfl, H., 1999. ^{1}H and ^{13}C NMR spectra for a series of arylmaleamic acids, arylmaleimides, arylsuccinamic acids and arylsuccinimides. Magn. Res. Chem. 37, 682–686.

Trybulski, E.J., Kramss, R.H., Mangano, R.M., Brabander, H.J., Francisco, G., 1992. The synthesis and structure activity relationships of enantiomerically pure hydroxylated oxotremorine derivatives. Bioorg. Med. Chem. Lett. 2, 827–832.

Walker, M.A., 1994. The Mitsunobu reaction: a novel method for the synthesis of bifunctional maleimide linkers. Tetrahedron Lett. 35, 665–668.